Research Article

Kinetic Investigation of Resistance to Islatravir Conferred by Mutations in HIV-1 Reverse Transcriptase

Nikita Zalenski, Brianna R. Meredith, Derek J. Savoie, Mohamed J. Naas, David J. Suo, Daniel Betancourt, Turner W. Seay, and Zucai Suo *

Department of Biomedical Sciences, *Florida State University College of Medicine, Tallahassee, FL 32306, USA*

Correspondence to Zucai Suo: *zucai.suo@med.fsu.edu (Z. Suo)*
https://doi.org/10.1016/j.jmb.2025.169100
Edited by Eric O. Freed

Abstract

Islatravir (EFdA) is a novel nucleoside reverse transcriptase translocation inhibitor (NRTTI) that potently blocks HIV-1 replication *in vivo*. Its unique structural features in contrast to nucleoside reverse transcriptase inhibitors (NRTIs), particularly the 4′-ethynyl and 3′-hydroxy groups, contribute to its high clinical potency. Once intracellularly activated to EFdA 5′-triphosphate (EFdA-TP), it competes with dATP for incorporation by HIV-1 reverse transcriptase (RT) during HIV-1 genomic replication. The 4′-ethynyl group of incorporated EFdA-MP interacts with a hydrophobic pocket of HIV-1 RT, hindering DNA translocation and terminating DNA synthesis. The M184V mutation, commonly associated with resistance to NRTIs such as lamivudine and emtricitabine, and the M184V/A114S mutations, both located within the hydrophobic pocket, were shown to reduce Islatravir susceptibility in cell-based viral resistance selection assays. To elucidate the mechanisms by which these mutations affect Islatravir inhibition, we employed pre-steady-state kinetics to investigate their impact on EFdA-TP incorporation by HIV-1 RT using both DNA and RNA templates. We found that M184V had a modest effect on EFdA-TP incorporation efficiency, increasing it 2-fold with the DNA template and decreasing it 3-fold with the RNA template. In contrast, M184V/A114S significantly inhibited EFdA-TP incorporation, reducing its incorporation efficiency 5.4-fold with the DNA template and 181-fold with the RNA template. These reductions were primarily attributable to corresponding decreases in EFdA-TP incorporation rate constants of 18-fold and 105-fold, respectively. These results suggest that, unlike FDA-approved NRTIs, the clinical efficacy of Islatravir, may not be substantially compromised by the M184V mutation alone but will be significantly reduced by the M184V/A114S mutations.

Introduction

HIV-1 reverse transcriptase (RT) is a multifunctional enzyme that catalyzes the reverse transcription of the viral RNA genome into double-stranded DNA prior to integration into the host genome.[1,2] This process involves both DNA-dependent DNA polymerase and RNA-dependent DNA polymerase activities of HIV-1 RT.[3–5] Additionally, HIV-1 RT possesses RNase H activity, which degrades the RNA template during reverse transcription.[1–3,6–8] Antiretroviral therapy for HIV-1 infection often includes the inhibition of HIV-1 RT, a critical enzyme for viral replication cycle. Two main classes of antiviral drugs, nucleoside/nucleotide reverse transcriptase inhibitors (NRTIs) and non-nucleoside reverse transcriptase inhibitors (NNRTIs), have been successfully developed in the past decades to target RT and prevent viral genome replication.[7,9–13] NRTIs are prodrugs that require

phosphorylation by cellular kinases to form their active triphosphate analogs. These activated NRTIs compete with natural dNTPs for incorporation into the growing viral DNA chain by HIV-1 RT. Currently FDA-approved NRTIs inhibit HIV-1 RT through chain termination due to their lack of a 3′-hydroxyl group, preventing further DNA elongation by HIV-1 RT. NNRTIs, often used in combination with NRTIs, bind to a non-competitive, allosteric site on RT which is opposite to the NRTI binding site, inducing conformational changes that impair the catalytic activities of HIV-1 RT.[7,12–14]

Islatravir, 4′-ethynyl-2-fluoro-2′-deoxyadenosine (EFdA), is a deoxyadenosine analogue, differs from FDA-approved NRTIs by retaining a 3′-hydroxyl group (Figure 1), which better matches and competes against natural dNTPs.[15] EFdA inhibits HIV-1 RT via a unique mechanism as a nucleoside reverse transcriptase translocation inhibitor (NRTTI).[15,16] The 4′-ethynyl (4′-E) group of EFdA forms hydrophobic interactions with the hydrophobic pocket of HIV-1 RT, comprised of residues A114, Y115, F160, M184, and D185 (Figure 2A).[17] These interactions prevent RT translocation following EFdA-TP incorporation.[17] Additionally, there are several residues (A113, A114, Y115, and Q151) that interact with the 3′-hydroxyl group of both natural dNTPs and EFdA-TP.[17,18] Islatravir demonstrates high potency against HIV-1, with an EC_{50} of 50 pM in cell culture assays.[15,19,20] This potent antiviral drug candidate is currently being evaluated in multiple Phase 3 clinical trials.

Treatment with HIV-1 RT inhibitors often leads to the emergence of drug-resistant HIV-1 strains through RT mutations. For example, the M184V substitution in HIV-1 RT is a well-established mechanism of resistance to several NRTIs such as lamivudine (3TC) and emtricitabine (FTC). This mutation occurs within the highly conserved YMDD motif found in several viral polymerases, including HIV-1 RT and HBV polymerase. Compared to wild-type (WT) HIV-1 RT, M184V confers very high levels of resistance (>100-fold) to lamivudine and emtricitabine.[19,21,22] Previous kinetic studies have shown that the M184V mutation primarily reduces the binding affinity of these NRTIs for the RT active site, leading to a significant decrease in their incorporation efficiency.[22,23] Additionally, previous viral resistance selection studies show that M184V is the most common substitution mutation to emerge after treatment with Islatravir, conferring ~7-fold loss in susceptibility to Islatravir. Another substitution mutation in HIV-1 RT, A114S, lowers the potency of Islatravir by ~2-fold but augments the resistance conferred by M184V resulting in an overall ~40-fold loss in susceptibility to Islatravir.[19] To elucidate the molecular mechanism of resistance conferred by the M184V and M184V/A114S mutations in HIV-1 RT, we employed pre-steady-state kinetic analysis to investigate the impact of these mutations on the nucleotide incorporation efficiency of EFdA-TP and dATP with both DNA and RNA templates. Our results provide a kinetic basis for the aforementioned decreases in Islatravir's potency by these HIV-1 RT mutations.

Material and Methods

Materials

[γ-^{32}P]ATP was purchased from Revvity Health Sciences, dATP from Fisher Scientific, and Biospin columns from Bio-Rad Laboratories. EFdA-TP was provided by Merck & Co., Inc. A DNA primer (21mer), a DNA template (27-DNA), and an RNA template (27-RNA) in Table 1 were purchased from Integrated DNA Technologies, Inc. and purified using polyacrylamide gel electrophoresis (PAGE).

DNA substrates

The primer, 21mer, was radiolabeled with [γ-^{32}P] ATP at 37 °C by T4 polynucleotide kinase.[24] The unreacted [γ-^{32}P] ATP was subsequently removed via a Bio-Spin 6 column (Bio-Rad).[25,26] To form 21/27-DNA and 21/27-RNA (Table 1), the primer and template were annealed in a 1:1.2 molar ratio in 20 mM Tris-HCl, pH 7.9 by heating at 95 °C for 5 min and slow cooling to room temperature over three hours.[27,28]

Proteins

Site-directed mutagenesis of WT HIV-1 RT expression plasmid[23] was used to generate expression plasmids encoding the M184V and M184V/A114S HIV-1 RT mutants at the Florida State University Department of Biological Science Core

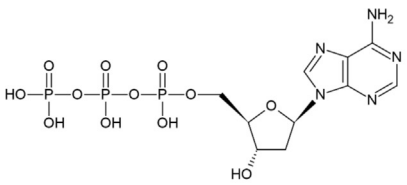

dATP

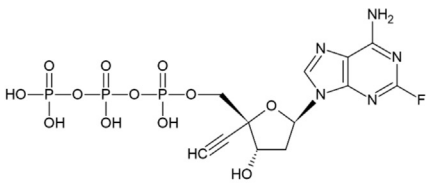

EFdA-TP

Figure 1. Chemical structures of dATP and 4′-ethynyl-2-fluoro-2′-deoxyadenosine 5′-triphosphate (EFdA-TP).

Facilities. The plasmids were subsequently sequenced at the same facilities to confirm the desired mutations. WT and mutant (M184V and M184V/A114S) HIV-1 RT proteins were individually expressed and purified as previously described.[23,29]

Pre-steady-state kinetic assays

Experiments were conducted at 37 °C using a rapid chemical quench-flow apparatus (KinTek) in the RT buffer (50 mM Tris-HCl, pH 7.9 at 37 °C, 10 mM $MgCl_2$, 50 mM NaCl, 0.1 mM EDTA, 10% glycerol, 5 mM DTT, 0.1 μg/ml BSA).[23] A preincubated solution of HIV-1 RT (300 nM) and 5′-^{32}P-labeled 21/27-DNA or 21/27-RNA (60 nM) was rapidly mixed with varying concentrations of dATP or EFdA-TP. After various times, the reactions were quenched with 0.37 M EDTA. All concentrations reported are final upon mixing unless stated otherwise. The reaction mixtures were denatured at 95 °C for 5 min and then separated by denaturing PAGE (17% acrylamide, 8 M urea, and 1x TBE buffer).[30,31] After drying, the gels were imaged with a Typhoon TRIO (GE Healthcare). ImageQuant (Molecular Dynamics) was used to analyze the gel images and background-corrected intensities were used to calculate incorporated products.[30,31] A non-linear regression software KaleidaGraph (Synergy) was used to fit the plot of product concentration versus time to a single-exponential equation,

$$[\text{Product}] = A[1 - e^{(-k_{obs}t)}] \quad (1)$$

where A and k_{obs} represent a reaction amplitude and an observed nucleotide incorporation rate constant, respectively. The k_{obs} was then plotted against nucleotide concentration to a hyperbolic equation,

$$k_{obs} = k_p[\text{dNTP}]/(K_d + [\text{dNTP}]) \quad (2)$$

where k_p is the maximal nucleotide incorporation rate constant, and K_d the apparent nucleotide binding equilibrium dissociation constant. Each kinetic assay was repeated three times. Standard error for the k_p/K_d was calculated using the standard error propagation equation for a ratio was calculated using the standard error propagation equation,

$$\sigma\frac{k_p}{K_d} = \frac{k_p}{K_d}\sqrt{\left(\frac{\sigma k_p}{k_p}\right)^2 + \left(\frac{\sigma K_d}{K_d}\right)^2} \quad (3)$$

Standard error for the selectivity factor, $(k_p/K_d)_{(\text{dATP})}/(k_p/K_d)_{(\text{EFdA-TP})}$, was calculated using the standard error propagation equation,

$$\sigma s = s\sqrt{\left(\frac{\sigma(k_p/K_d)_{(\text{dATP})}}{(k_p/K_d)_{(\text{dATP})}}\right)^2 + \left(\frac{\sigma(k_p/K_d)_{(\text{EFdA-TP})}}{(k_p/K_d)_{(\text{EFdA-TP})}}\right)^2} \quad (4)$$

where s is the selectivity factor.

Modeling

To model HIV-1 RT mutations structurally, we introduced the desired mutated residues into the pre-insertion ternary structure of wild-type HIV-1 RT (PDB 5J2M)[32] using COOT.[33] Assuming single residue mutations do not significantly perturb the overall protein backbone, the Cα positions of the mutated residues were maintained in positions similar to those of the wild-type HIV-1 RT structure (PDB 5J2M).[32]

Results and Discussion

Previous HIV-1 infected cell-based assays selecting for resistance to Islatravir have identified mutations in HIV-1 RT, specifically M184I, M184V, and the combined M184V/A114S.[19] Interestingly, M184V typically outcompetes the initially emerging M184I mutation and is the predominant mutation observed in patients experiencing virologic failure on NRTI treatment.[34] A114S has minimal impact on the polymerase activities of HIV-1 RT based on published steady state kinetic assays,[35] is very rarely seen clinically,[19,36] and only appears alongside M184V in the viral resistance selection assays.[19] For these reasons, we focused on the investigation of the kinetic basis for the reduced susceptibility to Islatravir conferred by the M184V and M184V/A114S HIV-1 RT mutants. Similar to our previous kinetic studies on antiviral and anticancer nucleoside analogs,[23,27,37–43] we utilized pre-steady-state kinetic assays (Material and Methods) to determine the kinetic parameters (k_p, K_d) for EFdA-TP incorporation onto 21/27-DNA (Table 1) by M184V (Figure 3, Table 2). The incorporation efficiency (k_p/K_d) of EFdA-TP and its standard error were then calculated (Table 2). Likewise, k_p, K_d, and k_p/K_d for EFdA-TP incorporation were determined with either 21/27-DNA or 21/27-RNA (Table 1) by WT or the M184V and M184V/A114S HIV-1 RT mutants and these pre-steady-state kinetic parameters were listed in Table 2. For comparison, the corresponding parameters for dATP incorporation were also determined (Table 2). To assess the relative nucleotide incorporation efficiencies with each enzyme and template, a selectivity factor, defined as $(k_p/K_d)_{(\text{dATP})}/(k_p/K_d)_{(\text{EFdA-TP})}$, was calculated (Table 2).

Interestingly, WT HIV-1 RT incorporated EFdA-TP and dATP with comparable efficiencies, exhibiting a small selectivity factor of 1.3 ± 0.7 with both DNA and RNA templates (Table 2). In comparison, our previous studies have determined the selectivity factors of 1.9 and 7.0 for the incorporation of FTC-TP and 3TC-TP relative to dCTP by WT HIV-1 RT, respectively.[23] These results suggest that EFdA-TP, like the known efficient substrates FTC-TP and 3TC-TP, was incorporated by WT HIV-1 RT with the efficiency (k_p/K_d)

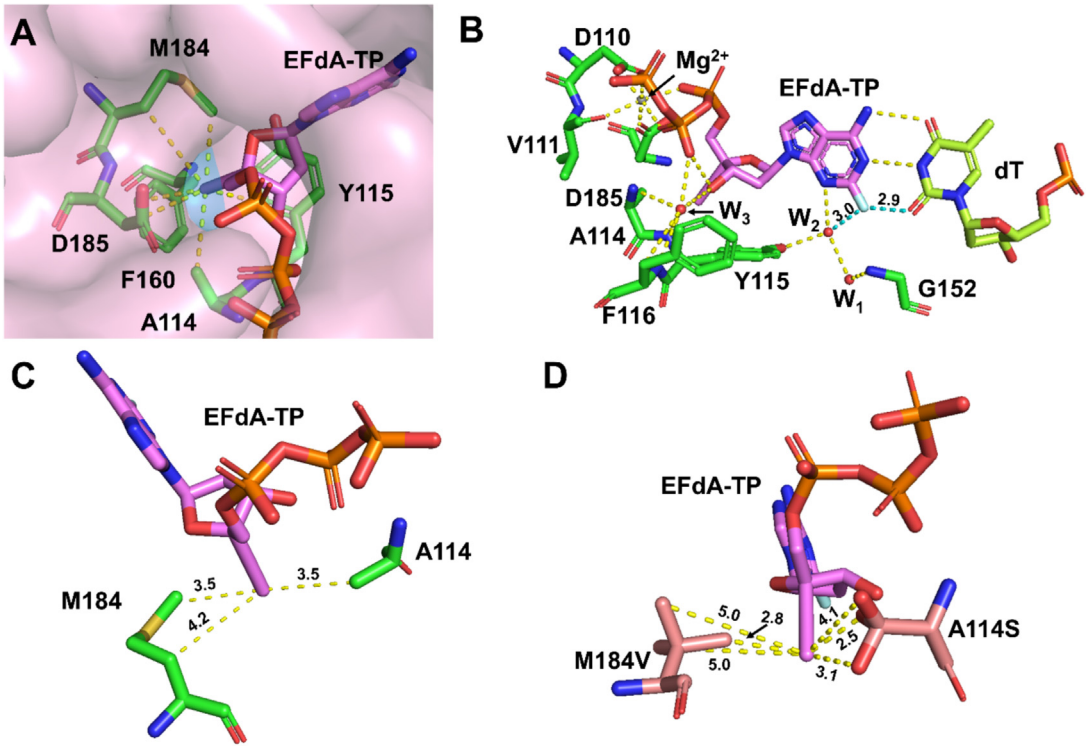

Figure 2. Zoomed view of the pre-insertion ternary complex of WT HIV-1 RT with DNA and EFdA-TP (PDB: 5J2M) and molecular modeling of mutated residues in the vicinity of the EFdA-TP. (A) Hydrophobic interactions (atoms within 4 Å; yellow dotted lines) of the 4′-ethynyl group of EFdA-TP within the hydrophobic pocket (light blue surface) near the polymerase active site. (B) Interactions (dotted lines) between EFdA-TP, the templating nucleotide dT, water molecules (red spheres, W_1, W_2, and W_3), Mg^{2+}, and active site residues of HIV-1 RT. The 2-fluoro atom of EFdA-TP (cyan) forms halogen bonds (cyan) with the 2-carbonyl oxygen atom of dT and the oxygen atom of W_2. (C) Zoomed view of the interactions between the 4′-ethynyl group of EFdA-TP with residues M184 and A114 of WT HIV-1 RT. (D) Interactions between the 4′-ethynyl group of EFdA-TP and modeled M184V and A114S rotamers. In Panels B-D, labeled distances are in Å.

Table 1 Double-stranded DNA substrates with either a DNA or an RNA template.

21/27-DNA	5′-ACAGTCCCTGTTCGGGCGCCG-3′ 3′-GTGTCAGGGACAAGCCCGCGGCTGGAT-5′
21/27-RNA	5′-ACAGTCCCTGTTCGGGCGCCG-3′ 3′-GUGUCAGGGACAAGCCCGCGGCUGGAU-5′

almost equal to that of the natural nucleotide dATP, explaining the observed high potency of Islatravir against HIV-1 viruses containing WT HIV-1 RT. In comparison, the k_p values of dATP are slightly higher than those of EFdA-TP while the K_d values for the two nucleotides are the opposite (Table 2). The lower K_d values of EFdA-TP indicate that EFdA-TP was bound slightly tighter than dATP in the nucleotide binding site (N-site) of HIV-1 RT. The 4′-ethynyl group of EFdA-TP binds and interacts with the well-defined hydrophobic pocket (Figure 2A) while other chemical groups of EFdA-TP engage in intense interactions with the templating nucleotide dTMP, Mg^{2+}, ordered water molecules, and active site residues (Figure 2B). Notably, the 2-fluoro atom of EFdA-TP forms a halogen bond with the 2-carbonyl oxygen atom of dTMP (Figure 2B), a feature that does not exist in the dATP:dTMP pair.

Relative to WT HIV-1 RT, the M184V mutation introduced template-dependent selectivity. With the RNA template, the selectivity factor was 1.1 ± 0.6, while with the DNA template, it was 1.0 ± 0.4 (Table 2). In comparison, previous steady-state kinetic analysis showed that the M184V mutation in HIV-1 RT reduces the catalytic efficiency (k_{cat}/K_m) of EFdA-TP incorporation with a DNA template by 1.2-fold.[35] Our observed small selectivity factors are not statistically significant from one another, indicating that the M184V mutation does not discriminate against EFdA-TP incorporation relative to dATP incorporation, with either DNA or RNA templates. It is worth noting that error ranges for selectivity factors are often not reported due to the accumulation of errors and because they may not be the most reliable metric for direct comparison between different selectivity factors. Selectivity factors serve as indicators of the relative

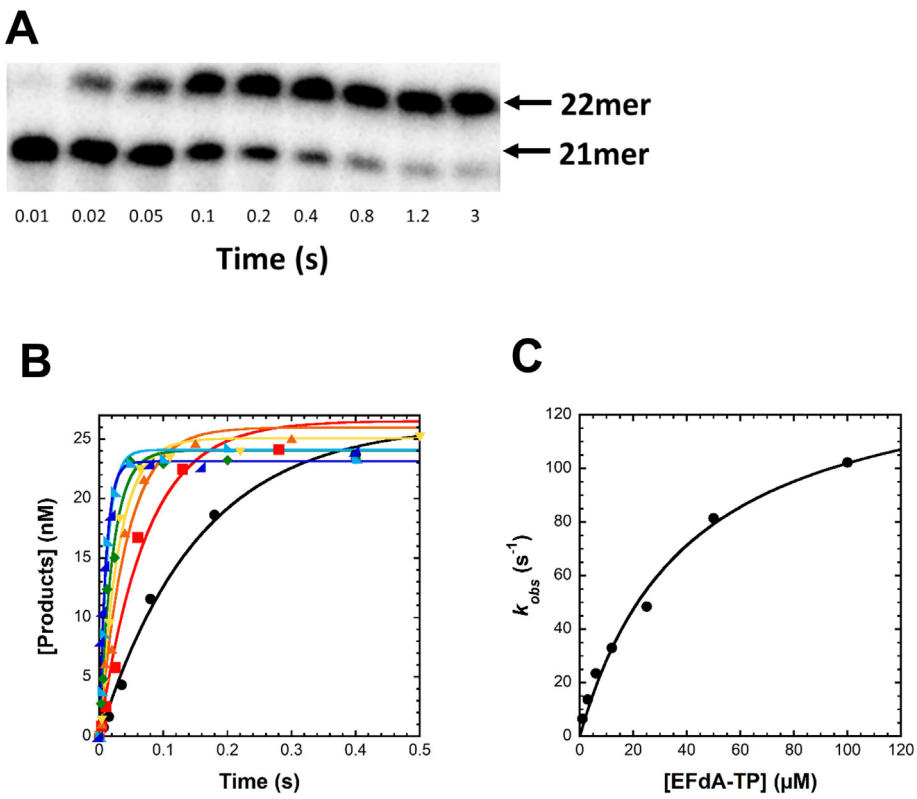

Figure 3. Determination of EFdA-TP incorporation kinetic parameters at 37 °C. A pre-incubated solution of 300 nM M184V HIV-1 RT and 60 nM 5′-^{32}P-labeled 21/27-DNA was mixed with increasing concentrations of EFdA-TP (1 μM, ●; 3 μM, ■; 6 μM, ▲; 12 μM, ▼; 25 μM, ◆; 50 μM, ◣; 100 μM, ◢) for various times before quenched with 0.37 M EDTA. (A) A representative Urea-PAGE gel of 4 μM EFdA-TP incorporation with DNA oligomer sizes indicated (right). (B) DNA product concentrations were plotted against time, and each time course was fit to a single-exponential equation (Eq. (1)) to yield k_{obs}. (C) The k_{obs} values were plotted against EFdA-TP concentration and the resulting plot was fit to a hyperbolic equation (Eq. (2)) to yield a k_p of 199 ± 25 s^{-1} and a K_d of 12 ± 3.4 μM for EFdA-TP incorporation.

differences in incorporation efficiency. Furthermore, M184V displayed a ~2-fold increase in the k_p/K_d value of EFdA-TP compared to WT HIV-1 RT with the DNA template, but a ~3-fold decrease with the RNA template (Table 2). These findings provide evidence that the M184V substitution overall modestly alters the inhibitory potency of Islatravir and underscore the intrinsic asymmetry of the active site of HIV-1 RT with respect to DNA and RNA templates.[44,45] The observed ~7-fold loss in susceptibility to Islatravir caused by M184V in the viral resistance selection assays[19] may be a function of thousands of rounds of EFdA-TP binding and incorporation during genomic viral replication, especially during plus strand synthesis. Comparatively, the M184V mutation decreases the incorporation efficiency of FTC-TP and 3TC-TP by 2,600- to 880-fold, respectively, with a DNA template.[23]

In contrast to M184V, the M184V/A114S mutant exhibited dramatically different selectivity for dATP over EFdA-TP, with selectivity factors of 3.3 ± 1.4 (DNA template) and 12 ± 5 (RNA template) (Table 2). With the DNA template, the incorporation efficiency (k_p/K_d) for dATP (3.9 ± 0.5 μM^{-1} s^{-1}) is ~3.3-fold higher than that of EFdA-TP (1.2 ± 0.5 μM^{-1} s^{-1}) (Table 2). The difference has been determined previously via steady-state kinetic assays to be 6.5-fold based on the k_{cat}/K_m values of dATP and EFdA-TP with a DNA template.[35] With the RNA template, dATP incorporation (0.59 ± 0.17 μM^{-1} s^{-1}) was ~13-fold more efficient than EFdA-TP incorporation (0.047 ± 0.01 4 μM^{-1} s^{-1}) (Table 2). These results indicate that the M184V/A114S mutations significantly reduced EFdA-TP incorporation efficiencies, resulting in a reduced frequency of EFdA-TP incorporation relative to dATP during HIV-1 genome replication and consequently contributing to the observed ~40-fold loss of Islatravir susceptibility conferred by the double mutations in HIV-1 RT.[19]

Relative to WT HIV-1 RT, the M184V/A114S mutant exhibited a substantial reduction in EFdA-TP incorporation efficiency: 181-fold with the RNA template (0.047 ± 0.014 μM^{-1} s^{-1} vs 8.5 ± 1.7 μM^{-1} s^{-1}) and 5.4-fold with the DNA template (1.2 ± 0.5 μM^{-1} s^{-1} vs 6.5 ± 3.2 μM^{-1} s^{-1}) (Table 2). These reductions in efficiency were primarily driven by corresponding decreases in k_p values of 105-fold

Table 2 Pre-steady-state kinetic parameters for incorporation of dATP or EFdA-TP onto 21/27-DNA or 21/27-RNA by WT, M184V, or M184V/A114S at 37 °C.

Substrate	HIV-1 RT	Nucleotide	k_p (s^{-1})	K_d (μM)	k_p/K_d (μM^{-1} s^{-1})[a]	Selectivity factor[b]
21/27-DNA (DNA template)	WT	dATP	227 ± 14	27 ± 4	8.4 ± 1.4	
		EFdA-TP	125 ± 23	19 ± 9	6.5 ± 3.2	1.3 ± 0.7
	M184V	dATP	321 ± 21	19 ± 3	17 ± 3	
		EFdA-TP	199 ± 25	12 ± 3	17 ± 5	1.0 ± 0.4
	M184V/A114S	dATP	108 ± 5	28 ± 3	3.9 ± 0.5	
		EFdA-TP	6.9 ± 0.7	5.9 ± 2.4	1.2 ± 0.5	3.3 ± 1.4
21/27-RNA (RNA template)	WT	dATP	248 ± 56	25 ± 9.8	9.9 ± 4.5	
		EFdA-TP	178 ± 16	21 ± 3.7	8.5 ± 1.7	1.2 ± 0.6
	M184V	dATP	206 ± 9.7	73 ± 9.7	2.8 ± 0.4	
		EFdA-TP	181 ± 9	69 ± 10	2.6 ± 0.4	1.1 ± 0.2
	M184V/A114S	dATP	61 ± 8	104 ± 27	0.59 ± 0.17	
		EFdA-TP	1.7 ± 0.2	36 ± 9.5	0.047 ± 0.014	12 ± 5

[a] Standard error was calculated based on Eq. (3) (Materials and Methods).
[b] $(k_p/K_d)_{(dATP)}/(k_p/K_d)_{(EFdA\text{-}TP)}$. The standard error for each selectivity factor was calculated based on Eq. (4) (Materials and Methods).

(RNA template: 1.7 ± 0.2 s^{-1} vs 178 ± 16 s^{-1}) and 18-fold (DNA template: 6.9 ± 0.7 s^{-1} vs 125 ± 23 s^{-1}) (Table 2). Similarly, dATP incorporation efficiency with the M184V/A114S mutant was reduced ~17-fold (RNA template: 0.59 ± 0.17 μM^{-1} s^{-1} vs 9.9 ± 4.5 μM^{-1} s^{-1}) and 2.2-fold (DNA template: 3.9 ± 0.5 μM^{-1} s^{-1} vs 8.4 ± 1.4 μM^{-1} s^{-1}) relative to WT HIV-1 RT, also reflecting decreases in k_p values of ~4-fold (61 ± 8 s^{-1} vs 248 ± 56 s^{-1}) and 2-fold (108 ± 5 s^{-1} vs 227 ± 14 s^{-1}), respectively (Table 2). In light of the established kinetic mechanism by which HIV-1 RT utilizes active site rearrangement to limit the rate of correct natural dNTP incorporation,[29,4,46,47] we speculate the M184V/A114S mutations induce significant structural alterations within the active site of the pre-insertion ternary complex, particularly when EFdA-TP is bound.

To analyze the HIV-1 RT mutations structurally, we modeled the desired mutated residues into the pre-insertion ternary structure of WT HIV-1 RT (PDB 5J2M)[32] using COOT (Materials and Methods).[33] Assuming single residue mutations do not significantly alter the amino acid residue locations, their Cα positions were thereby kept in similar positions to those in the WT HIV-1 RT structure.[32] The similar Cα positions allow us to visualize any potential steric clash after mutating a residue in WT RT structure. In addition, the side chains of mutated residues were allowed to exist in different rotamer conformations. the effective minimum distance between the 4′-E group of EFdA-TP and S114 was reduced to 2.5 Å (Figure 2D) from ~3.5 Å between A114 and 4′-E (Figure 2C). In the two alternative rotamers of S114, the distances were measured to be 3.1 and 4.1 Å (Figure 2D). Similarly, the effective minimum distance, which was estimated to be ~3.5 Å between the 4′-E group and M184 (Figure 2C), was reduced to be 2.8 Å when M184 was mutated to V184 (Figure 2D). In the two alternative rotamer conformations of V184, the two side chain carbons are equidistant to the 4′-E group with estimated distances of 5.0 Å each (Figure 2D). Given that the sum of the van der Waals radii of carbon and oxygen is ~3.2 Å, the M184V and M184V/A114S mutations likely cause a steric clash between the 4′-E group and the mutated residues (S114 and V184) within the hydrophobic pocket, resulting in slight adjustments to the positions of EFdA-TP and/or the mutated residues. These modeling predictions could be validated by structural analysis of the pre-insertion ternary complex of the M184V/A114S mutant bound to DNA and EFdA-TP, although such a structure is not currently available. Taken together, the M184V/A114S mutations create a tighter hydrophobic pocket around the bound EFdA-TP, leading to its higher binding affinity with the mutant than WT HIV-1 RT. Consistently, the K_d values of EFdA-TP are lower with the M184V/A114S mutant (5.9 ± 2.4 μM) than with WT HIV-1 RT (19 ± 9 μM) in the presence of the DNA template (Table 2). In comparison, the M184V mutation insignificantly lowered the K_d value of EFdA-TP (12 ± 3 μM vs 19 ± 9 μM) with the DNA template (Table 2). This means that the M184V mutation alone insignificantly alters the active site structure, and the 4′-E group repositions itself towards A114, leading to the observed minimal changes in EFdA-TP incorporation.[48] Consistently, besides the comparable K_d values, the k_p values of EFdA-TP incorporation (199 ± 25 s^{-1} vs 125 ± 23 s^{-1}) were not significantly changed by the M184V mutation relative to WT

HIV-1 RT with the DNA template (Table 2). Due to lack of a pre-insertion ternary structure with an RNA template, we could not speculate how EFdA-TP was bound and incorporated by WT HIV-1 RT or its mutants (M184V, M184V/A114S) in the presence of the RNA template (Table 1) and rationalize the corresponding kinetic parameters listed in Table 2.

In addition, unlike FDA-approved NRTIs, EFdA-MP, once incorporated at the primer 3′-terminus, possesses a 3′-OH group, permitting the incorporation of an additional dNTP before terminating DNA synthesis via a delayed chain termination mechanism.[15,16] HIV-1 RT mutations (M184V, M184V/A114S) likely alter this additional dNTP incorporation step, potentially resulting in distinct mechanisms of Islatravir resistance. Further kinetic and structural investigations are necessary to elucidate these differences between WT HIV-1 RT and these mutants.

Conclusion

Pre-steady-state kinetic assays were used to determine the kinetic basis for reduced Islatravir susceptibility conferred by the M184V and M184V/A114S mutations in HIV-1 RT. WT HIV-1 RT incorporated EFdA-TP and dATP with nearly equal k_p/K_d values. The M184V mutation increased EFdA-TP incorporation efficiency 2.6-fold with the DNA template but decreased it 3.3-fold with the RNA template. In contrast, the M184V/A114S mutations decreased EFdA-TP incorporation efficiency 5.4-fold with the DNA template and 181-fold with the RNA template, primarily due to corresponding decreases in k_p values of 18-fold and 105-fold, respectively. Despite these kinetic effects on EFdA-TP incorporation, the clinical relevance of these mutations in HIV-1 RT, identified in cell-based viral resistance selection assays, remains to be fully elucidated.

CRediT authorship contribution statement

Nikita Zalenski: Writing – original draft, Visualization, Validation, Methodology, Investigation, Formal analysis, Data curation. **Brianna R. Meredith:** Investigation, Formal analysis, Data curation. **Derek J. Savoie:** Methodology, Investigation. **Mohamed J. Naas:** Investigation. **David J. Suo:** Investigation. **Daniel Betancourt:** Validation, Investigation. **Turner W. Seay:** Investigation. **Zucai Suo:** Writing – review & editing, Writing – original draft, Supervision, Resources, Project administration, Methodology, Funding acquisition, Conceptualization.

DATA AVAILABILITY

Data will be made available on request.

Acknowledgements

This work was supported in part by a research grant from Investigator-Initiated Studies Program of Merck Sharp & Dohme LLC to Z.S. The opinions expressed in this paper are those of the authors and do not necessarily represent those of Merck Sharp & Dohme LLC.

Received 11 February 2025;
Accepted 20 March 2025;
Available online 24 March 2025

Keywords:
HIV-1 reverse transcriptase;
nucleoside reverse transcriptase translocation inhibitor;
Islatravir;
hydrophobic pocket;
pre-steady-state kinetic analysis

Abbreviations:
EFdA, 4′-Ethynyl-2-fluoro-2′-deoxyadenosine; 4′-E, 4′-ethynyl; EFdA-TP, EFdA 5′-triphosphate; HIV-1 RT, HIV-1 reverse transcriptase; NRTTI, nucleoside reverse transcriptase translocation inhibitor; NRTIs, nucleoside reverse transcriptase inhibitors; NNRTIs, non-nucleoside reverse transcriptase inhibitors; PAGE, polyacrylamide gel electrophoresis; TBE, Tris-Borate-EDTA

References

1. Hoffman, A.D., Banapour, B., Levy, J.A., (1985). Characterization of the AIDS-associated retrovirus reverse transcriptase and optimal conditions for its detection in virions. *Virology* **147**, 326–335.
2. Rey, M.A., Spire, B., Dormont, D., Barre-Sinoussi, F., Montagnier, L., Chermann, J.C., (1984). Characterization of the RNA dependent DNA polymerase of a new human T-lymphotropic retrovirus (lymphadenopathy associated virus). *Biochem. Biophys. Res. Commun.* **121**, 126–133.
3. Suo, Z., Johnson, K.A., (1997). RNA secondary structure switching during DNA synthesis catalyzed by HIV-1 reverse transcriptase. *Biochemistry* **36**, 14778–14785.
4. Suo, Z., Johnson, K.A., (1998). DNA secondary structure effects on DNA synthesis catalyzed by HIV-1 reverse transcriptase. *J. Biol. Chem.* **273**, 27259–27267.
5. Suo, Z., Lippard, S.J., Johnson, K.A., (1999). Single d (GpG)/cis-diammineplatinum(II) adduct-induced inhibition of DNA polymerization. *Biochemistry* **38**, 715–726.
6. Jacobo-Molina, A., Ding, J., Nanni, R.G., Clark Jr., A.D., Lu, X., Tantillo, C., Williams, R.L., Kamer, G., Ferris, A.L., Clark, P., et al., (1993). Crystal structure of human immunodeficiency virus type 1 reverse transcriptase

complexed with double-stranded DNA at 3.0 A resolution shows bent DNA. *PNAS* **90**, 6320–6324.
7. Sarafianos, S.G., Marchand, B., Das, K., Himmel, D.M., Parniak, M.A., Hughes, S.H., Arnold, E., (2009). Structure and function of HIV-1 reverse transcriptase: molecular mechanisms of polymerization and inhibition. *J. Mol. Biol.* **385**, 693–713.
8. Suo, Z., Johnson, K.A., (1997). Effect of RNA secondary structure on RNA cleavage catalyzed by HIV-1 reverse transcriptase. *Biochemistry* **36**, 12468–12476.
9. Arts, E.J., Hazuda, D.J., (2012). HIV-1 antiretroviral drug therapy. *Cold Spring Harb. Perspect. Med.* **2**, a007161.
10. De Clercq, E., (2009). The history of antiretrovirals: key discoveries over the past 25 years. *Rev. Med. Virol.* **19**, 287–299.
11. Kausar, S., Said Khan, F., Ishaq Mujeeb Ur Rehman, M., Akram, M., Riaz, M., Rasool, G., Hamid Khan, A., Saleem, I., Shamim, S., Malik, A., (2021). A review: mechanism of action of antiviral drugs. *Int. J. Immunopathol. Pharmacol.* **35**, 205873842110026.
12. De Clercq, E., (2024). Selected milestones in antiviral drug development. *Viruses* **16**, 169.
13. Yoshida, Y., Honma, M., Kimura, Y., Abe, H., (2021). Structure, synthesis and inhibition mechanism of nucleoside analogues as HIV-1 reverse transcriptase inhibitors (NRTIs). *ChemMedChem* **16**, 743–766.
14. Sluis-Cremer, N., Tachedjian, G., (2008). Mechanisms of inhibition of HIV replication by non-nucleoside reverse transcriptase inhibitors. *Virus Res.* **134**, 147–156.
15. Michailidis, E., Marchand, B., Kodama, E.N., Singh, K., Matsuoka, M., Kirby, K.A., Ryan, E.M., Sawani, A.M., Nagy, E., Ashida, N., et al., (2009). Mechanism of inhibition of HIV-1 reverse transcriptase by 4′-ethynyl-2-fluoro-2′-deoxyadenosine triphosphate, a translocation-defective reverse transcriptase inhibitor. *J. Biol. Chem.* **284**, 35681–35691.
16. Michailidis, E., Huber, A.D., Ryan, E.M., Ong, Y.T., Leslie, M.D., Matzek, K.B., Singh, K., Marchand, B., Hagedorn, A. N., Kirby, K.A., et al., (2014). 4′-Ethynyl-2-fluoro-2′-deoxyadenosine (EFdA) inhibits HIV-1 reverse transcriptase with multiple mechanisms. *J. Biol. Chem.* **289**, 24533–24548.
17. Salie, Z.L., Kirby, K.A., Michailidis, E., Marchand, B., Singh, K., Rohan, L.C., Kodama, E.N., Mitsuya, H., Parniak, M.A., Sarafianos, S.G., (2016). Structural basis of HIV inhibition by translocation-defective RT inhibitor 4′-ethynyl-2-fluoro-2′-deoxyadenosine (EFdA). *PNAS* **113**, 9274–9279.
18. Cases-Gonzalez, C.E., Menendez-Arias, L., (2005). Nucleotide specificity of HIV-1 reverse transcriptases with amino acid substitutions affecting Ala-114. *Biochem. J.* **387**, 221–229.
19. Diamond, T.L., Ngo, W., Xu, M., Goh, S.L., Rodriguez, S., Lai, M.T., Asante-Appiah, E., Grobler, J.A., (2022). Islatravir has a high barrier to resistance and exhibits a differentiated resistance profile from approved nucleoside reverse transcriptase inhibitors (NRTIs). *Antimicrob. Agents Chemother.* **66**, e0013322.
20. Lai, M.-T., Feng, M., Xu, M., Ngo, W., Diamond, T.L., Hwang, C., Grobler, J.A., Hazuda, D.J., Asante-Appiah, E., (2022). Doravirine and Islatravir have complementary resistance profiles and create a combination with a high barrier to resistance. *Antimicrob. Agents Chemother.* **66**, e02223–02221.
21. Schinazi, R.F., Lloyd Jr., R.M., Nguyen, M.H., Cannon, D. L., McMillan, A., Ilksoy, N., Chu, C.K., Liotta, D.C., Bazmi, H.Z., Mellors, J.W., (1993). Characterization of human immunodeficiency viruses resistant to oxathiolane-cytosine nucleosides. *Antimicrob. Agents Chemother.* **37**, 875–881.
22. Nastri, B.M., Pagliano, P., Zannella, C., Folliero, V., Masullo, A., Rinaldi, L., Galdiero, M., Franci, G., (2023). HIV and drug-resistant subtypes. *Microorganisms* **11**, 221.
23. Hung, M., Tokarsky, E.J., Lagpacan, L., Zhang, L., Suo, Z., Lansdon, E.B., (2019). Elucidating molecular interactions of L-nucleotides with HIV-1 reverse transcriptase and mechanism of M184V-caused drug resistance. *Commun. Biol.* **2**, 469.
24. Sherrer, S.M., Brown, J.A., Pack, L.R., Jasti, V.P., Fowler, J.D., Basu, A.K., Suo, Z., (2009). Mechanistic studies of the bypass of a bulky single-base lesion catalyzed by a Y-family DNA polymerase. *J. Biol. Chem.* **284**, 6379–6388.
25. Fiala, K.A., Sherrer, S.M., Brown, J.A., Suo, Z., (2008). Mechanistic consequences of temperature on DNA polymerization catalyzed by a Y-family DNA polymerase. *Nucleic Acids Res.* **36**, 1990–2001.
26. Brown, J.A., Fowler, J.D., Suo, Z., (2010). Kinetic basis of nucleotide selection employed by a protein template-dependent DNA polymerase. *Biochemistry* **49**, 5504–5510.
27. Fowler, J.D., Brown, J.A., Johnson, K.A., Suo, Z., (2008). Kinetic investigation of the inhibitory effect of gemcitabine on DNA polymerization catalyzed by human mitochondrial DNA polymerase. *J. Biol. Chem.* **283**, 15339–15348.
28. Brown, J.A., Suo, Z., (2009). Elucidating the kinetic mechanism of DNA polymerization catalyzed by Sulfolobus solfataricus P2 DNA polymerase B1. *Biochemistry* **48**, 7502–7511.
29. Suo, Z., Johnson, K.A., (1997). Effect of RNA secondary structure on the kinetics of DNA synthesis catalyzed by HIV-1 reverse transcriptase. *Biochemistry* **36**, 12459–12467.
30. Zhang, L., Brown, J.A., Newmister, S.A., Suo, Z., (2009). Polymerization fidelity of a replicative DNA polymerase from the hyperthermophilic archaeon Sulfolobus solfataricus P2. *Biochemistry* **48**, 7492–7501.
31. Brown, J.A., Newmister, S.A., Fiala, K.A., Suo, Z., (2008). Mechanism of double-base lesion bypass catalyzed by a Y-family DNA polymerase. *Nucleic Acids Res.* **36**, 3867–3878.
32. Salie, Z.L., Kirby, K.A., Michailidis, E., Marchand, B., Singh, K., Rohan, L.C., Kodama, E.N., Mitsuya, H., Parniak, M.A., Sarafianos, S.G., (2016). Structural basis of HIV inhibition by translocation-defective RT inhibitor 4'-ethynyl-2-fluoro-2'-deoxyadenosine (EFdA). *PNAS* **113**, 9274–9279.
33. Emsley, P., Lohkamp, B., Scott, W.G., Cowtan, K., (2010). Features and development of Coot. *Acta Crystallogr. D Biol. Crystallogr.* **66**, 486–501.
34. Keulen, W., Boucher, C., Berkhout, B., (1996). Nucleotide substitution patterns can predict the requirements for drug-resistance of HIV-1 proteins. *Antiviral Res.* **31**, 45–57.
35. Cilento, M.E., Reeve, A.B., Michailidis, E., Ilina, T.V., Nagy, E., Mitsuya, H., Parniak, M.A., Tedbury, P.R., Sarafianos, S.G., (2021). Development of Human Immunodeficiency Virus Type 1 Resistance to 4'-Ethynyl-2-Fluoro-2'-

Deoxyadenosine Starting with Wild-Type or Nucleoside Reverse Transcriptase Inhibitor-Resistant Strains. *Antimicrob. Agents Chemother.* **65**, e0116721.
36. Rhee, S.Y., Gonzales, M.J., Kantor, R., Betts, B.J., Ravela, J., Shafer, R.W., (2003). Human immunodeficiency virus reverse transcriptase and protease sequence database. *Nucleic Acids Res.* **31**, 298–303.
37. Vyas, R., Reed, A.J., Raper, A.T., Zahurancik, W.J., Wallenmeyer, P.C., Suo, Z., (2017). Structural basis for the D-stereoselectivity of human DNA polymerase beta. *Nucleic Acids Res.* **45**, 6228–6237.
38. Gaur, V., Vyas, R., Fowler, J.D., Efthimiopoulos, G., Feng, J. Y., Suo, Z., (2014). Structural and kinetic insights into binding and incorporation of L-nucleotide analogs by a Y-family DNA polymerase. *Nucleic Acids Res.* **42**, 9984–9995.
39. Vyas, R., Zahurancik, W.J., Suo, Z., (2014). Structural basis for the binding and incorporation of nucleotide analogs with L-stereochemistry by human DNA polymerase lambda. *PNAS* **111**, E3033–E3042.
40. Brown, J.A., Pack, L.R., Fowler, J.D., Suo, Z., (2011). Pre-steady-state kinetic analysis of the incorporation of anti-HIV nucleotide analogs catalyzed by human X- and Y-family DNA polymerases. *Antimicrob. Agents Chemother.* **55**, 276–283.
41. Brown, J.A., Pack, L.R., Fowler, J.D., Suo, Z., (2012). Presteady state kinetic investigation of the incorporation of anti-hepatitis B nucleotide analogues catalyzed by noncanonical human DNA polymerases. *Chem. Res. Toxicol.* **25**, 225–233.
42. Suo, Z., Johnson, K.A., (1998). Selective inhibition of HIV-1 reverse transcriptase by an antiviral inhibitor, (R)-9-(2-phosphonylmethoxypropyl)adenine. *J. Biol. Chem.* **273**, 27250–27258.
43. Johnson, A.A., Ray, A.S., Hanes, J., Suo, Z., Colacino, J. M., Anderson, K.S., Johnson, K.A., (2001). Toxicity of antiviral nucleoside analogs and the human mitochondrial DNA polymerase. *J. Biol. Chem.* **276**, 40847–40857.
44. Wei, X., Liang, C., Gotte, M., Wainberg, M.A., (2003). Negative effect of the M184V mutation in HIV-1 reverse transcriptase on initiation of viral DNA synthesis. *Virology* **311**, 202–212.
45. Tian, L., Kim, M.S., Li, H., Wang, J., Yang, W., (2018). Structure of HIV-1 reverse transcriptase cleaving RNA in an RNA/DNA hybrid. *PNAS* **115**, 507–512.
46. Kati, W.M., Johnson, K.A., Jerva, L.F., Anderson, K.S., (1992). Mechanism and fidelity of HIV reverse transcriptase. *J. Biol. Chem.* **267**, 25988–25997.
47. Raper, A.T., Reed, A.J., Suo, Z., (2018). Kinetic mechanism of DNA polymerases: contributions of conformational dynamics and a third divalent metal ion. *Chem. Rev.* **118**, 6000–6025.
48. Takamatsu, Y., Das, D., Kohgo, S., Hayashi, H., Delino, N. S., Sarafianos, S.G., Mitsuya, H., Maeda, K., (2018). The high genetic barrier of EFdA/MK-8591 stems from strong interactions with the active site of drug-resistant HIV-1 reverse transcriptase. *Cell Chem. Biol.* **25**, 1268–1278. e1263.